Strong decays of excited 2^+ charmed mesons

Xiao-Ze Tan[1], Tianhong Wang[1,*], Yue Jiang[1], Qiang Li[2], Lei Huo,[1] and Guo-Li Wang[1,3,4]

[1]*School of Physics, Harbin Institute of Technology, Harbin 150001, China*
[2]*School of Physical Science and Technology, Northwestern Polytechnical University, Xi'an 710129, China*
[3]*Department of Physics, Hebei University, Baoding 071002, China*
[4]*Hebei Key Laboratory of High-precision Computation and Application of Quantum Field Theory,
Baoding 071002, China*

The new charmed resonance $D_2^*(3000)$ was observed by the LHCb Collaboration in B decays. In this paper, by assigning it as four possible excited states of the 2^+ family, we use the instantaneous Bethe-Salpeter method to calculate their Okubo-Zweig-Iizuka-allowed two-body strong decays. The results of 1^3F_2 and 3^3P_2 states deviate from the present experimental observation while 2^3P_2 and 2^3F_2 are in the error range. Our study also reveals that the widths of these states depend strongly on the masses. Due to the large uncertainties and different mass input, variable models get inconsistent conclusions at the moment. The analysis in this work can provide essential assistance for future measurements and investigations.

I. INTRODUCTION

During the last decades, many charmed mesons have been found and cataloged [1]. With increasing results published, more attention has moved to heavy and excited states. These new states not only enrich the spectrum of D mesons but also offer us an opportunity to explore their properties from related decays. In 2013 and 2016, the LHCb Collaboration announced their observations of several charmed resonances around 3000 MeV, including $D_J(3000)$, $D_J^*(3000)$, and $D_2^*(3000)$ [2,3]. $D_J(3000)$ and $D_J^*(3000)$ are observed from $D^*\pi$ and $D\pi$ mass spectrum. Their assignments and strong decays have been widely discussed [4–9]. Our previous works prefer they are $2P(1^{+\prime})$ and $2P(0^+)$ states, respectively [10,11]. The $D_2^*(3000)$ is observed in the B decays, whose mass and width are

$$M(D_2^*(3000)^0) = 3214 \pm 29 \pm 33 \pm 36 \text{ MeV},$$
$$\Gamma(D_2^*(3000)^0) = 186 \pm 38 \pm 34 \pm 63 \text{ MeV}. \quad (1)$$

While the nature of this state is uncertain, it was generally considered as an excited state of the 2^+ family.

---
*Corresponding author.
thwang@hit.edu.cn

We summarize some theoretical predictions of the 2^+ spectrum in Table I. $D_2^*(2460)$, as the ground state 1^3P_2, was observed and examined by many experiments [1]. Our previous work calculated and compared its strong decays with other theoretical studies [7,12–15]. For the higher 2^3P_2, 1^3F_2, 3^3P_2, and 2^3F_2 states their predicted masses range from around 2900 MeV to 3500 MeV. Due to the large uncertainties in the preliminary measurement of $D_2^*(3000)$, all these four states cannot be ruled out easily from the candidate list.

To identify the $D_2^*(3000)$ from these possible assignments, an investigation on their decay behaviors at the experimental mass is necessary. Usually, the Okubo-Zweig-Iizuka (OZI) allowed strong decays are dominant for charmed mesons. Some efforts about their decays have been made and several theoretical methods were applied, including heavy quark effective theory (HQET) [8,21], the quark pair creation (QPC) model (also named as the $^3P_0$ model) [4,9,17,22], and the chiral quark model [20,23]. Significant discrepancies still exist between different works and the comparison will be discussed later in Sec. III.

Since the relativistic effects in heavy-light mesons are not negligible, especially for excited states, we use the wave functions obtained by the instantaneous Bethe-Salpeter (BS) approach [24,25] to calculate the OZI allowed two-body strong decays. The BS method has been applied successfully in many previous works [26–36] and the relativistic corrections in the heavy flavor mesons are well considered [37]. When the light pseudoscalar mesons are involved in the final states, the reduction formula, partially conserved axial-vector current (PCAC) relation, and low-energy theorem are used to depict the quark-meson

TABLE I. Theoretical predicted masses of 2^+ charmed mesons (MeV).

|	Ebert [16]	Godfrey [7]	Song [9] and Wang [17]	Badalian [18]	Patel [19]	Ni [20]
1^3P_2	2460	2502	2468	2466	2462	2475
2^3P_2	3012	2957	2884	2968	2985	2955
1^3F_2	3090	3132	3053	3059	3080	3096
3^3P_2	...	3353	3234	3264	3402	...
2^3F_2	...	3490	3364	3430	3494	...

coupling. Since PCAC is inapplicable when the final light meson is a vector, for instance ρ, ω, and K^*, an effective Lagrangian is adopted instead [38,39].

The rest of the paper is organized as follows: In Sec. II we briefly construct BS wave functions of 2^+ state. Then we derive the theoretical formalism of the strong decays with the PCAC relation and the effective Lagrangian method. In Sec. III the numerical results and detailed discussions are presented. Finally, we summarize our work in Sec. IV.

II. THEORETICAL FORMALISM

We first introduce the BS wave functions used in this work. The general form of 2^+ wave function is constructed as [28,31]

$$
\begin{aligned}
\varphi_{2^+}(q_\perp) = \epsilon_{\mu\nu}q_\perp^\mu q_\perp^\nu &\left[f_1(q_\perp) + \frac{\not{P}}{M}f_2(q_\perp) \right.\\
&\left. + \frac{\not{q}_\perp}{M}f_3(q_\perp) + \frac{\not{P}\not{q}_\perp}{M^2}f_4(q_\perp) \right]\\
&+ M\epsilon_{\mu\nu}\gamma^\mu q_\perp^\nu \left[f_5(q_\perp) + \frac{\not{P}}{M}f_6(q_\perp) \right.\\
&\left. + \frac{\not{q}_\perp}{M}f_7(q_\perp) + \frac{\not{P}\not{q}_\perp}{M^2}f_8(q_\perp) \right],
\end{aligned}
\tag{2}
$$
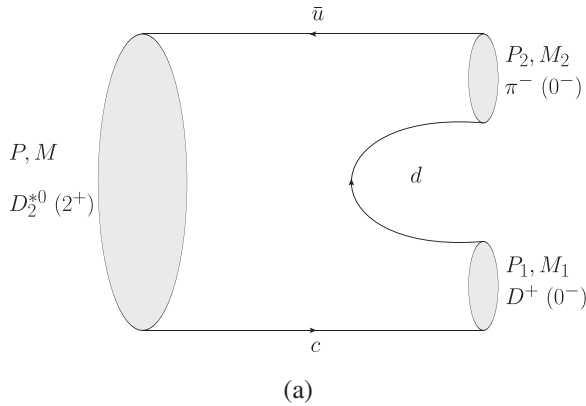
where M and P are the mass and momentum of the meson, q is the relative momentum of the quark and antiquark in the meson and $q_\perp$ is denoted as $q - \frac{P\cdot q}{M^2}P$, $\epsilon_{\mu\nu}$ is the polarization tensor, and f_i are the functions of $q_\perp$; their numerical values are obtained by solving the full Salpeter equations [26,40]. Moreover, the wave functions f_i in Eq. (2) are independent, which are constrained by

$$
\begin{aligned}
f_1(q_\perp) &= \frac{q_\perp^2 f_3(\omega_1 + \omega_2) + 2M^2 f_5\omega_2}{M(m_1\omega_2 + m_2\omega_1)},\\
f_2(q_\perp) &= \frac{q_\perp^2 f_4(\omega_1 - \omega_2) + 2M^2 f_6\omega_2}{M(m_1\omega_2 + m_2\omega_1)},\\
f_7(q_\perp) &= \frac{M(\omega_1 - \omega_2)}{m_1\omega_2 + m_2\omega_1}f_5,\\
f_8(q_\perp) &= \frac{M(\omega_1 + \omega_2)}{m_1\omega_2 + m_2\omega_1}f_6,
\end{aligned}
\tag{3}
$$

where m_i is the quark/antiquark mass, $\omega_i = \sqrt{m_i^2 - q_\perp^2}$, and $q_\perp^2 = -|\vec{q}|^2$ in the rest frame of the meson.

The review of instantaneous approximation and the action kernel adopted in this paper was given in our previous work [41]. Due to the approximation, our previous results showed that the predicted mass spectrum for excited heavy-light mesons may not fit the experimental data very well. Thus we follow our previous works [10,30,35] to use the physical mass as an input parameter to solve the BS wave functions for each state. As we did formerly [11], only the dominant positive-energy part of wave functions $\varphi^{++} = \Lambda_1^+ \frac{\not{P}}{M}\varphi\frac{\not{P}}{M}\Lambda_2^+$ are kept in the following calculation, which was explained in Ref. [41] in detail.

Taking $D_2^* \to D^+\pi^-$ as an example, the Feynman diagram of two-body strong decay is shown in Fig. 1. By using the reduction formula, the corresponding transition matrix element has the form
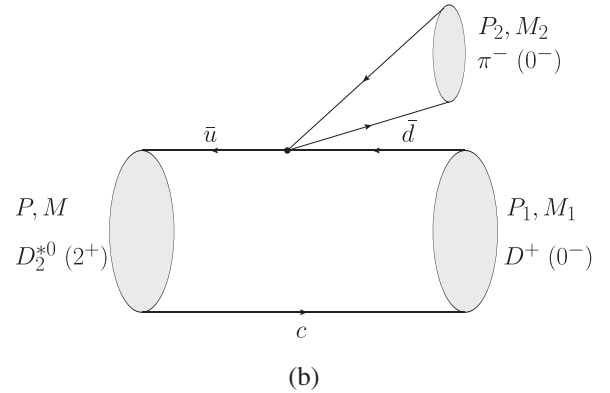

FIG. 1. Feynman diagram of the OZI-allowed two-body strong decay, taking $D_2^{*0} \to D^+\pi^-$ for example. (a) Leading order diagram (b) Approximate diagram.

$\langle D^+(P_1)\pi^-(P_2)|D_2^{*0}(P)\rangle$

$$= \int d^4x e^{iP_2 \cdot x}(M_\pi^2 - P_2^2)\langle D^+(P_1)|\phi_\pi(x)|D_2^{*0}(P)\rangle, \quad (4)$$

in which ϕ_π is the light pseudoscalar meson field. By using the PCAC relation, the field is expressed as

$$\phi_\pi(x) = \frac{1}{M_\pi^2 f_\pi}\partial^\mu(\bar{u}\gamma_\mu\gamma_5 d), \quad (5)$$

where f_π is the decay constant of π. Then, by using the low-energy approximation, the transition amplitude in momentum space can be derived as [42]

$\langle D^+(P_1)\pi^-(P_2)|D_2^{*0}(P)\rangle$

$$\approx -i\frac{P_2^\mu}{f_\pi}(2\pi)^4\delta^4(P - P_1 - P_2)\langle D^+(P_1)|\bar{u}\gamma_\mu\gamma_5 d|D_2^{*0}(P)\rangle. \quad (6)$$

Besides the PCAC relation, the same transition amplitude can be obtained by introducing an effective Lagrangian [10,38,39]

$$\mathcal{L}_{qqP} = \frac{g}{\sqrt{2}f_h}\bar{q}_i\gamma^\xi\gamma^5 q_j\partial_\xi\phi_{ij}, \quad (7)$$

where

$$\phi_{ij} = \sqrt{2}\begin{bmatrix} \frac{1}{\sqrt{2}}\pi^0 + \frac{1}{\sqrt{6}}\eta & \pi^+ & K^+ \\ \pi^- & -\frac{1}{\sqrt{2}}\pi^0 + \frac{1}{\sqrt{6}}\eta & K^0 \\ K^- & K^0 & -\frac{2}{\sqrt{6}}\eta \end{bmatrix}, \quad (8)$$

denotes the chiral field of the light pseudoscalar meson, g is the quark-meson coupling constant and f_h is the decay constant.

For further numerical calculation, in the Mandelstam formalism [43] we can write the hadronic transition amplitude as the overlapping integration over the relativistic wave functions of the initial and final mesons [42]

$$\mathcal{M} = -i\frac{P_2^\mu}{f_\pi}\langle D^+(P_1)|\bar{u}\gamma_\mu\gamma_5 d|D_2^{*0}(P)\rangle$$

$$= -i\frac{P_2^\mu}{f_\pi}\int\frac{d^3q}{(2\pi)^3}\text{Tr}\left[\bar{\varphi}_{P_1}^{++}(q_{1\perp})\frac{\not{P}}{M}\varphi_P^{++}(q_\perp)\gamma_\mu\gamma_5\right], \quad (9)$$

where φ^{++} and $\bar{\varphi}^{++}$ are the positive part of BS wave function and its Dirac adjoint form, and the quark-antiquark relative momenta in the initial and final meson have the relation $q_1 = q - \frac{m_c}{m_c+m_d}P_1$.

When the final light meson is η or η' instead of π, we also consider the $\eta - \eta'$ mixing [1]

$$\begin{pmatrix} \eta \\ \eta' \end{pmatrix} = R^T(\theta_\eta)\begin{pmatrix} \eta_8 \\ \eta_1 \end{pmatrix}, \quad (10)$$

where

$$\eta_8 = \frac{1}{\sqrt{6}}(u\bar{u} + d\bar{d} - 2s\bar{s}),$$

$$\eta_1 = \frac{1}{\sqrt{3}}(u\bar{u} + d\bar{d} + s\bar{s}). \quad (11)$$

$R(\theta)$ or $R^T(\theta)$ is the mixing matrix defined as

$$R(\theta) = \begin{pmatrix} \cos\theta & \sin\theta \\ -\sin\theta & \cos\theta \end{pmatrix},$$

$$R^T(\theta) = \begin{pmatrix} \cos\theta & -\sin\theta \\ \sin\theta & \cos\theta \end{pmatrix}. \quad (12)$$

We choose the mixing angle $\theta_\eta = -11.3°$ [1] in this work. By extracting the coefficient of mixing, the transition amplitudes with η/η' involved are

$$\mathcal{M}(\eta) = -iP_2^\mu M_\eta^2\left(\frac{\cos\theta_\eta}{\sqrt{6}f_{\eta_8}M_{\eta_8}^2} - \frac{\sin\theta_\eta}{\sqrt{3}f_{\eta_1}M_{\eta_1}^2}\right)$$

$$\times \langle D^{(*)}(P_1)|\bar{u}\gamma_\mu\gamma_5 u|D_2^*(P)\rangle,$$

$$\mathcal{M}(\eta') = -iP_2^\mu M_{\eta'}^2\left(\frac{\sin\theta_\eta}{\sqrt{6}f_{\eta_8}M_{\eta_8}^2} + \frac{\cos\theta_\eta}{\sqrt{3}f_{\eta_1}M_{\eta_1}^2}\right)$$

$$\times \langle D^{(*)}(P_1)|\bar{u}\gamma_\mu\gamma_5 u|D_2^*(P)\rangle. \quad (13)$$

When the final light meson is a vector, such as ρ or ω, the PCAC rule is not valid. Thus we adopt the effective Lagrangian method to derive the transition amplitude. The effective Lagrangian of light vector meson is given by [10,38,39]

$$\mathcal{L}_{qqV} = \sum_j \bar{q}_j\left(a\gamma_\mu + \frac{ib}{2m_j}\sigma_{\mu\nu}P_2^\nu\right)V^\mu q_j, \quad (14)$$

where m_j is the constitute quark mass [we take approximation $m_j = (m_q + m_{\bar{q}})/2$ in this work], $\sigma_{\mu\nu} = \frac{i}{2}[\gamma_\mu,\gamma_\nu]$; V^μ is the light vector meson field, and the parameters $a = -3$ and $b = 2$ denote the vector and tensor coupling strength [39], respectively. Then we use Eq. (14) directly to get the vertex of the light vector and reach the transition amplitude

$$\mathcal{M} = -i\int\frac{d^3q}{(2\pi)^3}\text{Tr}\left[\bar{\varphi}_{P_1}^{++}(q_{1\perp})\frac{\not{P}}{M}\varphi_P^{++}(q_\perp)\right.$$

$$\left.\times\left(a\gamma_\mu + \frac{ib}{2m_j}\sigma_{\mu\nu}P_2^\nu\right)\varepsilon_2^\mu\right]. \quad (15)$$

In the possible strong decays of $D_2^*(3000)$, 1^+ and 2^- states of D mesons are also involved in the final state. In the

heavy quark limit($m_Q \to \infty$), the coupling of spin S and orbital angular momentum L no longer describes the physical states well for these heavy-light states. The $^1P_1$—$^3P_1$ and $^1D_2$—$^3D_2$ mixing are needed. We take the total angular momentum of the light quark in the mesons $\vec{j}_l = \vec{L} + \vec{s}_q$ (s_q is the light-quark spin) to identify the physical doublet. The mixing relations are given by [16,33,44,45]

$$
\begin{pmatrix} |J^P = 1^+, j_l = 3/2\rangle \\ |J^P = 1^+, j_l = 1/2\rangle \end{pmatrix} = R(\theta_{1P}) \begin{pmatrix} |^1P_1\rangle \\ |^3P_1\rangle \end{pmatrix},
$$

$$
\begin{pmatrix} |J^P = 2^-, j_l = 5/2\rangle \\ |J^P = 2^-, j_l = 3/2\rangle \end{pmatrix} = R(\theta_{1D}) \begin{pmatrix} |^1D_2\rangle \\ |^3D_2\rangle \end{pmatrix}, \qquad (16)
$$

where the ideal mixing angles $\theta_{1P} = \arctan(\sqrt{1/2}) \approx 35.3°$ and $\theta_{1D} = \arctan(\sqrt{2/3}) \approx 39.2°$ in the heavy-quark limit are adopted. We notice that varying mixing angles could make difference to the decay widths. The dependence of corresponding partial widths on mixing angle will be discussed later.

In our calculation, the Salpeter equations for $^1P_1$ and $^3P_1$ ($^1D_2$ and $^3D_2$) states are solved individually and the state messes are mixing by the physical masses values

$$
\begin{pmatrix} m_{^1P_1}^2 & \delta \\ \delta & m_{^3P_1}^2 \end{pmatrix} = R^T(\theta_{1P}) \begin{pmatrix} m_{3/2}^2 & 0 \\ 0 & m_{1/2}^2 \end{pmatrix} R(\theta_{1P}),
$$

$$
\begin{pmatrix} m_{^1D_2}^2 & \delta \\ \delta & m_{^3D_2}^2 \end{pmatrix} = R^T(\theta_{1D}) \begin{pmatrix} m_{5/2}^2 & 0 \\ 0 & m_{3/2}^2 \end{pmatrix} R(\theta_{1D}). \quad (17)
$$

According to Refs. [33,41,46,47], we specify $D_1(2420)/D_{s1}(2536)$ as $|j_l = 3/2\rangle$ and $D_1(2430)/D_{s1}(2460)$ as $|j_l = 1/2\rangle$ for 1^+ state, $D_2(2740)$ as $|j_l = 5/2\rangle$ and $D_2(2780)$ as $|j_l = 3/2\rangle$ for 2^- state within this paper.

By performing the integration and trace in Eqs. (9) and (15), the amplitudes of all possible channels within the present study can be simplified as

$$
\mathcal{M}_{(2^+ \to 0^- 0^-)} = \frac{1}{f_{P_2}} t_1 \epsilon_{\mu\nu} P_1^\mu P_1^\nu,
$$

$$
\mathcal{M}_{(2^+ \to 0^- 1^-)} = t_2 \epsilon_{\mu\nu} \epsilon_{2\alpha} P_\beta P_{1\gamma} P_1^\mu \varepsilon^{\nu\alpha\beta\gamma},
$$

$$
\mathcal{M}_{(2^+ \to 0^+ 1^-)} = \epsilon_{\mu\nu} \epsilon_{2\alpha} (t_3 P_1^\mu P_1^\nu P^\alpha + t_4 P_1^\nu g^{\mu\alpha}),
$$

$$
\mathcal{M}_{(2^+ \to 1^- 0^-)} = \frac{i}{f_{P_2}} t_5 \epsilon_{\mu\nu} \epsilon_{1\alpha} P_\beta P_{1\gamma} P_1^\mu \varepsilon^{\nu\alpha\beta\gamma},
$$

$$
\mathcal{M}_{(2^+ \to 1^- 1^-)} = \epsilon_{\mu\nu} \epsilon_{1\alpha} \epsilon_{2\beta} [P_1^\mu (t_6 P_1^\nu P^\alpha P^\beta + t_7 P_1^\nu g^{\alpha\beta} + t_8 P^\alpha g^{\nu\beta} + t_9 P^\beta g^{\nu\alpha}) + t_{10} g^{\mu\alpha} g^{\nu\beta}],
$$

$$
\mathcal{M}_{(2^+ \to 1^{+(\prime)} 0^-)} = \frac{i}{f_{P_2}} \epsilon_{\mu\nu} \epsilon_{1\alpha} (t_{11}^{(\prime)} P_1^\mu P_1^\nu P^\alpha + t_{12}^{(\prime)} P_1^\mu g^{\nu\alpha}),
$$

$$
\mathcal{M}_{(2^+ \to 1^{+(\prime)} 1^-)} = \epsilon_{\mu\nu} \epsilon_{1\alpha} \epsilon_{2\beta} [P_1^\mu \varepsilon^{\nu\alpha\beta\gamma} (t_{13}^{(\prime)} P_\gamma + t_{14}^{(\prime)} P_{1\gamma}) + t_{15}^{(\prime)} P_1^\mu P^\beta P_\gamma P_{1\delta} \varepsilon^{\nu\alpha\gamma\delta} + t_{16}^{(\prime)} P_\gamma P_{1\delta} g^{\mu\alpha} \varepsilon^{\nu\beta\gamma\delta} + t_{17}^{(\prime)} P_1^\mu P_1^\nu P_\gamma P_{1\delta} \varepsilon^{\alpha\beta\gamma\delta}],
$$

$$
\mathcal{M}_{(2^+ \to 2^+ 0^-)} = \frac{i}{f_{P_2}} \epsilon_{\mu\nu} \epsilon_{1\alpha\beta} P_\gamma P_{1\delta} \varepsilon^{\nu\beta\gamma\delta} (t_{18} P_1^\mu P^\alpha + t_{19} g^{\mu\alpha}),
$$

$$
\mathcal{M}_{(2^+ \to 2^{-(\prime)} 0^-)} = \frac{1}{f_{P_2}} \epsilon_{\mu\nu} \epsilon_{1\alpha\beta} [P_1^\mu P^\alpha (t_{20}^{(\prime)} P_1^\nu P^\beta + t_{21}^{(\prime)} g^{\nu\beta}) + t_{22}^{(\prime)} g^{\mu\alpha} g^{\nu\beta}], \qquad (18)
$$

in which t_i are the form factors achieved by integrating over the wave functions for specific channels, $\varepsilon^{\alpha\beta\gamma\delta}$ is the Levi-Civita symbol, ϵ, ϵ_1, and ϵ_2 are the polarization tensors or vectors of corresponding states. For convenience, we define

$$
\Pi_{\alpha\beta} = -g_{\alpha\beta} + \frac{P_\alpha P_\beta}{M^2}, \qquad (19)
$$

where P and M are the momentum and mass of the corresponding meson. Then, the completeness relations of polarization vector and tensor are given by

$$
\sum_r \epsilon_\mu^{(r)} \epsilon_{\mu'}^{*(r)} = \Pi_{\mu\mu'},
$$

$$
\sum_r \epsilon_{\mu\nu}^{(r)} \epsilon_{\mu'\nu'}^{*(r)} = \frac{1}{2}(\Pi_{\mu\mu'} \Pi_{\nu\nu'} + \Pi_{\mu\nu'} \Pi_{\nu\mu'}) - \frac{1}{3} \Pi_{\mu\nu} \Pi_{\mu'\nu'}. \quad (20)
$$

The two-body decay width can be achieved by

$$
\Gamma = \frac{1}{8\pi} \frac{|\vec{P}_1|}{M^2} \frac{1}{2J+1} \sum_r |\mathcal{M}|^2, \qquad (21)
$$

TABLE II. The strong decay widths (MeV) of $D_2^*(3000)^0$ as different possible assignments. The present experiment mass $M = 3214$ MeV is used for each assignment here.

	2^3P_2	3^3P_2	1^3F_2	2^3F_2		2^3P_2	3^3P_2	1^3F_2	2^3F_2
$D^+\pi^-$	7.19	1.28	13.9	4.85	$D^{*+}\pi^-$	5.78	1.81	8.02	1.91
$D^0\pi^0$	3.66	0.635	6.93	2.49	$D^{*0}\pi^0$	2.94	0.882	4.06	0.987
$D^0\eta$	0.167	0.0258	1.81	0.520	$D^{*0}\eta$	0.0393	0.042	0.95	0.191
$D^0\eta'$	0.458	0.000679	5.01	0.590	$D^{*0}\eta'$	0.747	0.00699	1.46	0.139
$D_0(2550)^+\pi^-$	28.9	0.107	10.2	1.31	$D_1^*(2600)^+\pi^-$	38.3	0.0458	4.96	0.274
$D_0(2550)^0\pi^0$	14.5	0.0565	5.17	0.681	$D_1^*(2600)^0\pi^0$	19.3	0.0245	2.54	0.144
$D_0(2550)^0\eta$	0.575	0.0418	0.262	0.0286	$D_1^*(2600)^0\eta$	0.0991	0.00298	0.0159	0.000275
$D_s^+K^-$	1.18	0.738	8.77	1.58	$D_s^{*+}K^-$	0.762	0.841	2.97	0.509
$D^+\rho^-$	4.76	0.879	0.753	0.458	$D^{*+}\rho^-$	12.5	3.40	2.61	0.690
$D^0\rho^0$	2.51	0.439	0.384	0.242	$D^{*0}\rho^0$	6.38	1.72	1.43	0.368
$D^0\omega^0$	2.35	0.417	0.402	0.245	$D^{*0}\omega^0$	6.44	1.71	1.44	0.358
$D_s^+K^{*-}$	0.381	0.315	0.306	0.0851	$D_s^{*+}K^{*-}$	6.88	2.62	0.118	0.0311
$D_0^*(2400)^+\rho^-$	5.18	0.00184	0.251	0.00212	$D_2^*(2460)^+\pi^-$	3.29	0.0708	1.46	0.0465
$D_0^*(2400)^0\rho^0$	4.03	0.0328	0.23	0.00503	$D_2^*(2460)^0\pi^0$	1.68	0.0331	0.743	0.0218
$D_0^*(2400)^0\omega^0$	3.87	0.0209	0.198	0.00392	$D_2^*(2460)^0\eta$	0.136	0.00494	0.102	0.00230
$D_{s0}^*(2317)^+K^{*-}$	0.0551	9.48×10^{-5}	0.00790	4.29×10^{-5}	$D_{s2}(2573)^+K^-$	0.0982	0.0165	0.140	0.0168
$D_1(2420)^+\pi^-$	27.6	0.0916	75.8	8.52	$D_1(2430)^+\pi^-$	24.7	0.340	64.9	7.40
$D_1(2420)^0\pi^0$	14.3	0.0473	38.2	4.43	$D_1(2430)^0\pi^0$	12.8	0.192	32.8	3.90
$D_1(2420)^0\eta$	0.835	0.00784	10.1	0.695	$D_1(2430)^0\eta$	0.746	0.0174	8.70	0.595
$D_{s1}(2536)^+K^-$	1.21	0.0105	31.8	2.27	$D_{s1}(2460)^+K^-$	3.53	0.0646	46.0	3.93
$D_1(2420)^+\rho^-$	2.34	0.0142	11.6	0.205	$D_1(2430)^+\rho^-$	0.472	0.00360	3.07	0.0490
$D_1(2420)^0\rho^0$	1.48	0.00887	7.32	0.128	$D_1(2430)^0\rho^0$	0.358	0.00262	2.34	0.0358
$D_1(2420)^0\omega$	0.673	0.00572	3.41	0.0515	$D_1(2430)^0\omega$	0.0868	0.000823	0.579	0.00784
$D_2(2740)^+\pi^-$	3.78	0.0223	123	3.60	$D_2(2780)^+\pi^-$	2.42	0.0461	113	2.70
$D_2(2740)^0\pi^0$	1.91	0.00914	61.2	1.84	$D_2(2780)^0\pi^0$	1.22	0.0229	56.6	1.39
Total	285.6	19.1	778.0	60.5					

where $|\vec{P}_1| = \sqrt{\lambda(M^2, M_1^2, M_2^2)}/2M$ is the momentum of the final charmed meson,[1] $J = 2$ is the spin quantum number of the initial 2^+ state.

III. RESULTS AND DISCUSSIONS

In this work, the Cornell potential is taken to solve the BS equations of the 2^+ states numerically. Within the instantaneous approximation, the Cornell potential in momentum space has the following form [41]

$$I(\vec{q}) = V_s(\vec{q}) + \gamma_0 \otimes \gamma^0[V_v(\vec{q}) + V_0], \qquad (22)$$

where V_0 is a free parameter fixed by the physical masses of corresponding mesons, and the linear confinement item V_s and the one-gluon exchange Coulomb-type item V_v are

$$V_s(\vec{q}) = -\frac{\lambda}{\alpha}(2\pi)^3\delta^3(\vec{q}) + \frac{8\pi\lambda}{(\vec{q}^2 + \alpha^2)^2},$$

$$V_v(\vec{q}) = -\frac{16\pi\alpha_s(\vec{q})}{3(\vec{q}^2 + \alpha^2)}. \qquad (23)$$

---

[1]Källén function: $\lambda(x,y,z) = x^2 + y^2 + z^2 - 2xy - 2yz - 2zx$.

The coupling constant α_s is running

$$\alpha_s(\vec{q}) = \frac{12\pi}{27}\frac{1}{\ln\left(e + \frac{\vec{q}^2}{\Lambda_{QCD}^2}\right)}, \qquad (24)$$

where $e = 2.7183$.

The parameters adopted in the numerical calculation are listed as follows [31]:

$$m_u = 0.305\,\text{GeV}, \quad m_d = 0,311\,\text{GeV}, \quad m_c = 1.62\,\text{GeV},$$

$$m_s = 0.500\,\text{GeV}, \quad \alpha = 0.060\,\text{GeV}, \quad \lambda = 0.210\,\text{GeV}^2,$$

$$\Lambda_{QCD} = 0.270\,\text{GeV}, \quad f_\pi = 0.130\,\text{GeV}, \quad f_K = 0.156\,\text{GeV},$$

$$f_{\eta_1} = 1.07 f_\pi, \qquad f_{\eta_8} = 1.26 f_\pi,$$

$$M_{\eta_1} = 0.923\,\text{GeV}, \quad M_{\eta_8} = 0.604\,\text{GeV}.$$

For the doublet of 2^- charmed states, the masses $m_{D_2(2740)} = 2.747$ GeV and $m_{D_2(2780)} = 2.780$ GeV are used. The masses values of other involved mesons are taken from Ref. [1].

Before presenting our results, a remark is in order. When we solve the wave functions, the 2^+ states actually are the

mixture of several partial waves [48]. Within this work, to avoid confusion, we will not discuss this mixing in detail and still use pure P or F waves to mark each 2^+ state.

Within our calculation, the wave functions of each state are acquired by fixed on the experimental mass, which also gives the same phase space for every assignment. The total and partial widths of $D_2^*(3000)$ with possible assignments

are presented in Table II. In the four possible candidates, $D_2^*(3000)$ as 1^3F_2 has the largest total width in our prediction, which is about 778.0 MeV and much exceeds the upper limit of present experimental results. The channels of $D\pi$, $D^*\pi$, D_sK, $D_1(2420)/D_1(2430)\pi(\eta)$, $D_{s1}(2536)/D_{s1}(2460)K$, and $D_2(2740)/D_2(2780)\pi$ contribute much to the total width. In these dominant channels,
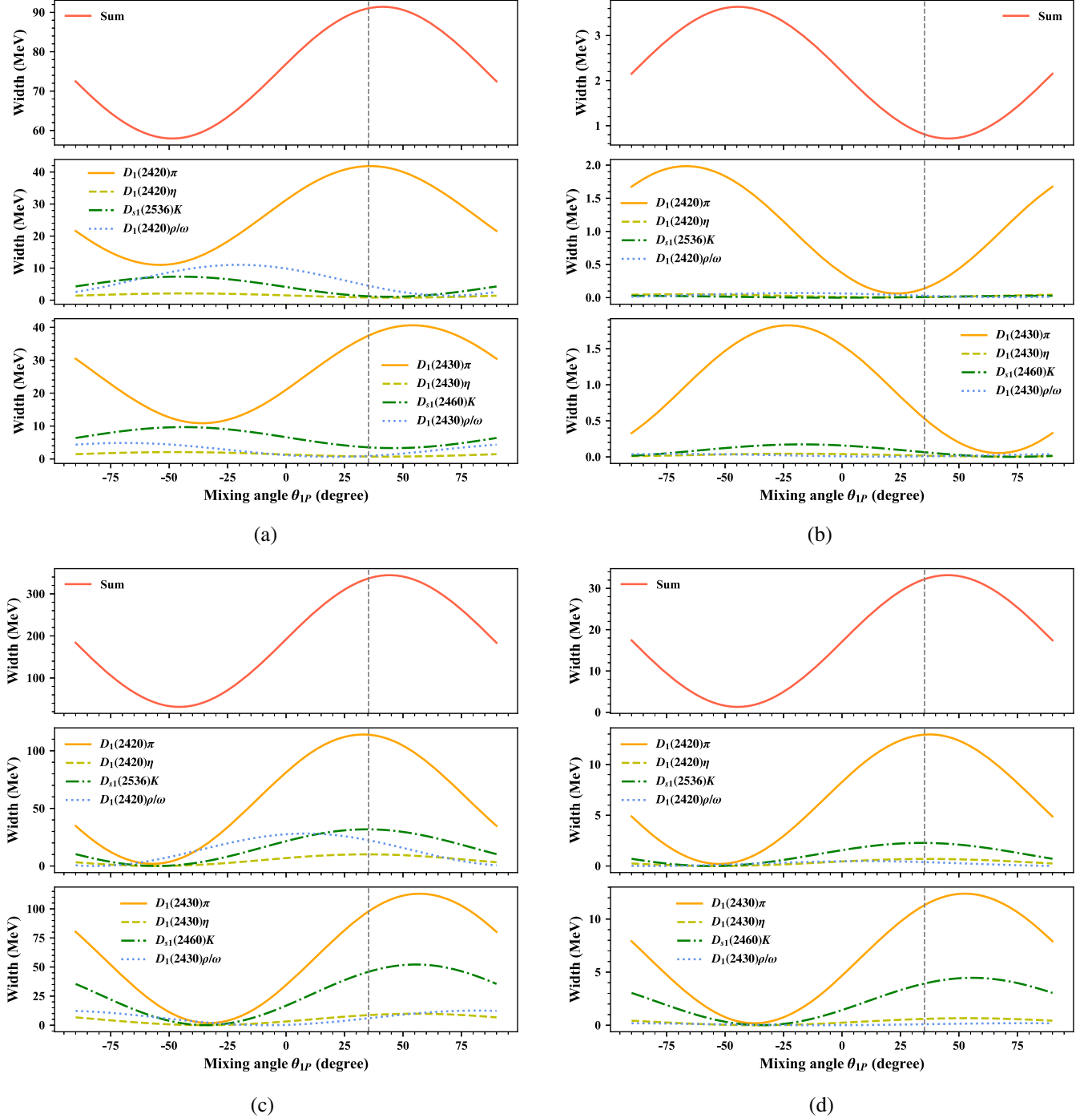

FIG. 2. The dependence of partial widths of channels involving final $D_1(2420)/D_{s1}(2536)$ or $D_1(2430)/D_{s1}(2460)$ mesons on mixing angle θ_{1P}. The vertical dashed line indicates the ideal mixing angle $\theta_{1P} = \arctan(\sqrt{1/2}) \approx 35.3°$. (a) $D_2^*(3000)^0$ as 2^3P_2 state, (b) $D_2^*(3000)^0$ as 3^3P_2 state, (c) $D_2^*(3000)^0$ as 1^3F_2 state, (d) $D_2^*(3000)^0$ as 2^3F_2 state.

the branching fraction of $D\pi$ mode is about 3%. And the partial width ratio of $D^*\pi$ to $D\pi$ are given by

$$\frac{\Gamma[1^3F_2 \to D^*\pi]}{\Gamma[1^3F_2 \to D\pi]} \approx 0.58. \tag{25}$$

In the case of 2^3P_2 state, the total width is estimated to be 285.6 MeV, which is larger than the observational value but still in the error range. The dominant channels include $D\pi$, $D^*\pi$, $D\rho(\omega)$, $D^*\rho(\omega)$, $D_s^*K^*$, and $D_1(2420)/D_1(2430)\pi$. Our predicted branching fractions of $D\pi$ for 2^3P_2 is about 4%. The partial width ratio between $D^*\pi$ and $D\pi$ is

$$\frac{\Gamma[2^3P_2 \to D^*\pi]}{\Gamma[2^3P_2 \to D\pi]} \approx 0.80. \tag{26}$$

The total widths of 2^3F_2 and 3^3P_2 are about 61 MeV and 19.1 MeV, respectively. The width of 2^3F_2 reaches the lower limit while the result of 3^3P_2 does not. The channels $D\pi$, $D^*\pi$, $D_1(2420)/D_1(2430)\pi$, and $D_2(2740)/D_2(2780)\pi$ give the main contribution to the width of 2^3F_2, while 3^3P_2 dominantly decay into $D\pi$, $D^*\pi$, $D^*\rho(\omega)$, and $D_s^*K^*$. The branching fractions of $D\pi$ for 2^3F_2 and 3^3P_2 are 12% and 10%, respectively. The corresponding partial width ratios are
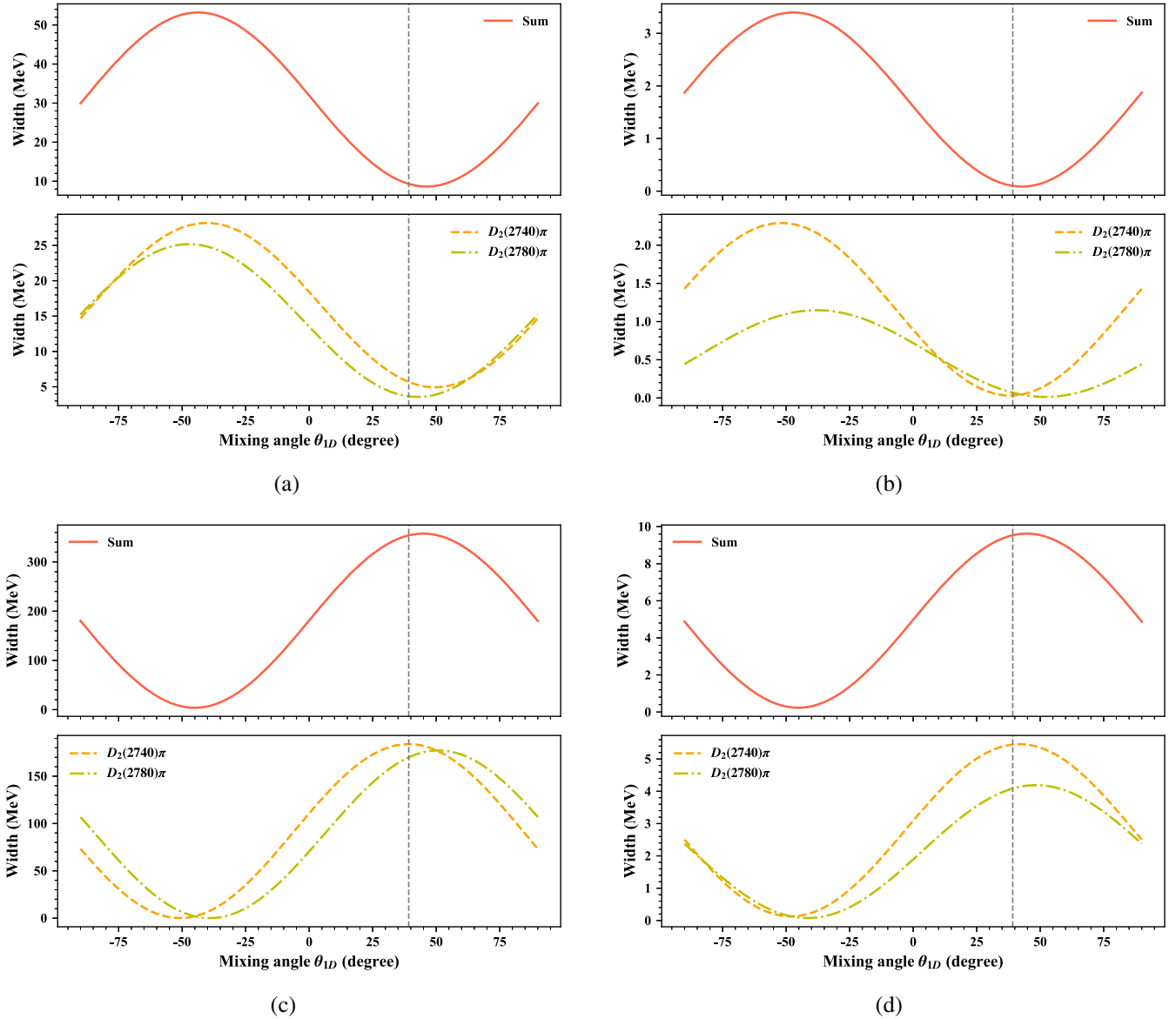

FIG. 3. The dependence of partial widths of channels involving final $D_2(2740)$ or $D_2(2780)$ mesons on mixing angle θ_{1D}. The vertical dashed line indicates the ideal mixing angle $\theta_{1D} = \arctan(\sqrt{2/3}) \approx 39.2°$. (a) $D_2^*(3000)^0$ as 2^3P_2 state, (b) $D_2^*(3000)^0$ as 3^3P_2 state, (c) $D_2^*(3000)^0$ as 1^3F_2 state, (d) $D_2^*(3000)^0$ as 2^3F_2 state.
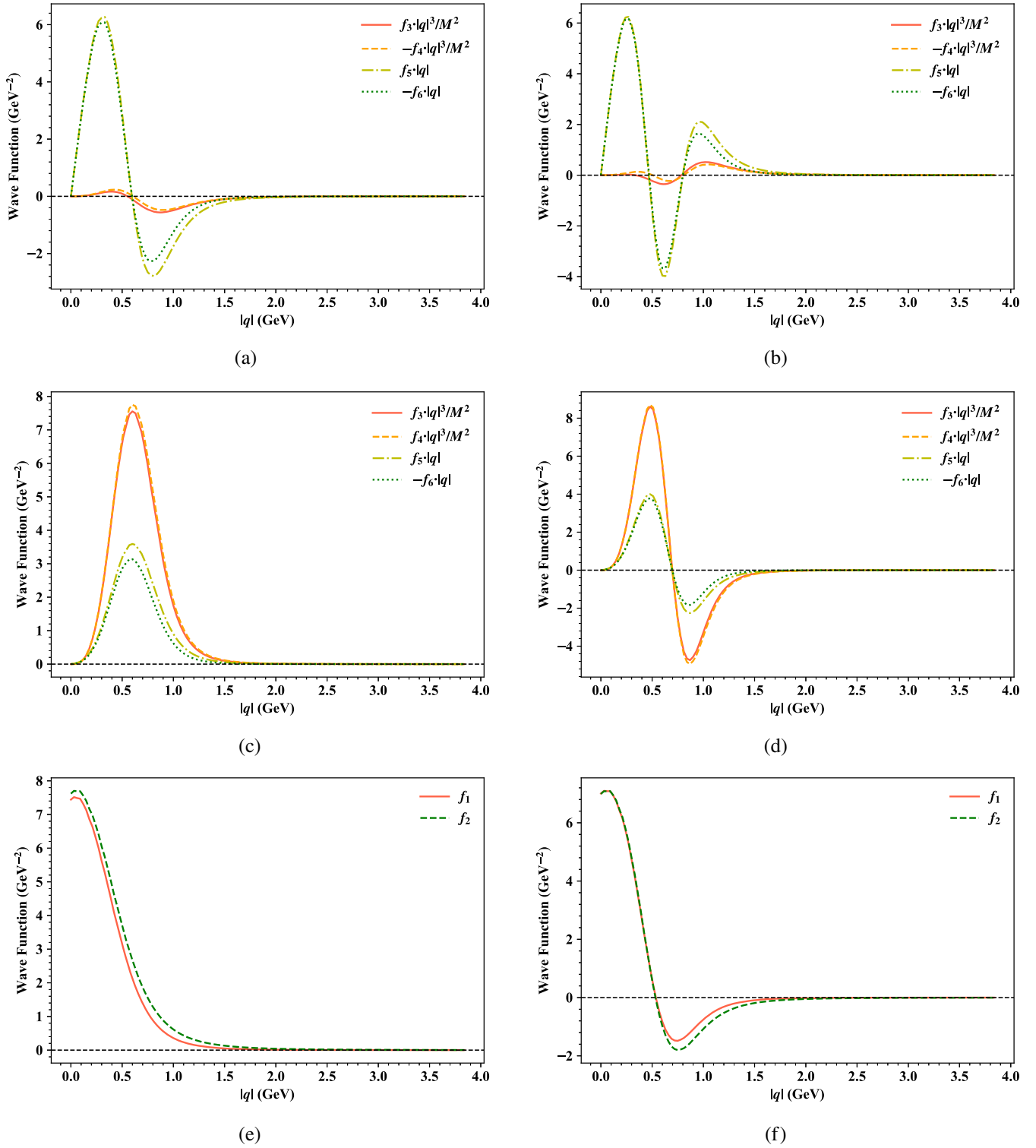
FIG. 4. Some wave functions of $D_2^*(3000)$ as different assignments, D^0 as 1^1S_0, and $D_0(2550)^0$ as 2^1S_0. (a) $D_2^*(3000)^0$ as 2^3P_2 state (b) $D_2^*(3000)^0$ as 3^3P_2 state, (c) $D_2^*(3000)^0$ as 1^3F_2 state, (d) $D_2^*(3000)^0$ as 2^3F_2 state, (e) D^0 as 1^1S_0, (f) $D_0(2550)^0$ as 2^1S_0.

TABLE III. Different theoretical predicted widths (MeV) for charmed 2^+ states. The values in parentheses are the masses used in the corresponding references. Others without parentheses use $M = 3214$ MeV.

	Sun [4]	Xiao [23]	Godfrey [7]	Song [9]	Yu [22]	Wang [17]	Ni [20]	Ours
2^3P_2	47(3008)	150(3020)	114(2957)	68.89(2884)	442.36	...	193.4(2955)	285.57
1^3F_2	136(3008)	900(3100)	243(3132)	222.02(3053)	220.05	...	722(3096)	778.10
3^3P_2	...	...	116(3353)	...	62.57	102.4(3234)	...	19.13
2^3F_2	...	...	223(3490)	...	32.09	302.2(3364)	...	60.53

$$\frac{\Gamma[2^3F_2 \to D^*\pi]}{\Gamma[2^3F_2 \to D\pi]} \approx 0.39, \tag{27}$$

$$\frac{\Gamma[3^3P_2 \to D^*\pi]}{\Gamma[3^3P_2 \to D\pi]} \approx 1.41. \tag{28}$$

We notice that $D\pi$ mode is appreciable for all four candidates, which is consistent with present experimental observations. The widths of channels involving $D_1(2420)/D_1(2430)$, $D_{s1}(2536)/D_{s1}(2460)$, and $D_2(2740)/D_2(2780)$ are also considerable especially for 2^3P_2, 3^3P_2, and 2^3F_2 states. In addition, the partial width ratios of $D\pi$ to $D^*\pi$ are different for these candidates, which could be useful for future experimental test.

The results in Table II are calculated by using ideal mixing and the divergence of the mixing angle could give large corrections. Thus, we show the dependence of partial widths on mixing angles θ_{1P} and θ_{1D} in Figs. 2 and 3. As 1^3F_2 and 2^3F_2 states, the widths could be reduced by up to about 640 MeV and 40 MeV in total, respectively if the negative angles for both θ_{1P} and θ_{1D} are chosen. In the instance of 2^3P_2 and 3^3P_2 states, the total widths could approximately increase by 10 MeV and 6 MeV, respectively when the negative mixing angles are appointed. The mixing has been discussed in our previous works [41,49] and ideal mixing is valid for $D_1(2420)$ and $D_1(2430)$. Here we only show the sensitive dependence between partial widths and mixing angle. In the following discussion, we keep using the results of ideal mixing for consistency.

Although all four assignments are calculated by fitting the same mass value $M = 3214$ MeV, which gives equivalent phase space for the same channels, the decay behaviors of these states are quite different. In our work, the discrepancy of total widths for different assignments can be explained by the special structure of wave functions. The numerical wave functions of $D_2^*(3000)$ with different states and $D(1^1S_0)/D(2^1S_0)$ in final states are shown as Fig. 4. 2^3P_2, 3^3P_2, 2^3F_2 as an example, and 2^1S_0 states have nodes and the wave function values alter the sign after nodes, which could lead to cancellation (or enhancement) in the overlapping integration. For example, the width of $D(2^3P_2) \to D(2^1S_0)\pi$ is larger than $D(2^3P_2) \to D(1^1S_0)\pi$. Both 2^3P_2 and 2^1S_0 have one node, which finally enhance the integral. However, in the case of 3^3P_2, the structure of two nodes eventually gives contrary behavior with the same

two channels. For 1^3F_2 and 2^3F_2, since the shape of wave functions are different (f_3, f_4, and f_5 always have the same sign for n^3F_2, while f_3 and f_4 have the same sign for n^3P_2), the widths of $D(2^1S_0)\pi$ are smaller than $D(1^1S_0)\pi$. In general, 1^3F_2 and 2^3P_2 states reach larger widths with less cancellation, while 2^3F_2 and 3^3P_2 behave oppositely. It also illustrate that the correction from higher internal momentum q of mesons is non-negligible.

Finally, we list the full widths of excited 2^+ states from some other models in Table III for comparison. Different methods give inconsistent results at present because the mass values used in these references are varied. Considering the predicted mass spectrum of 2^+ charmed states, we show our total widths of 2^3P_2, 1^3F_2, 3^3P_2, and 2^3F_2 change with masses in the range of 2850–3250 MeV and 3100–3500 MeV, respectively in Fig. 5. We can find that the widths vary widely along with the masses. At $M = 2900$–3000 MeV and $M = 3050$–3150 MeV, the 2^3P_2 and 1^3F_2 states reach the total width of 21 MeV $\sim$ 69 MeV and 427 MeV $\sim$ 649 MeV subsequently, which shows a similar trend with the results of Refs. [7] and [9]. In a similar manner, the widths of the 3^3P_2 and 2^3F_2 states are in the range of 22 MeV–49 MeV and 196 MeV–416 MeV at the masses $M = 3250$–3350 MeV and $M = 3350$–3450 MeV, which is very roughly close to the value of Refs. [7] and [17], respectively. Finally, when comparing our results with
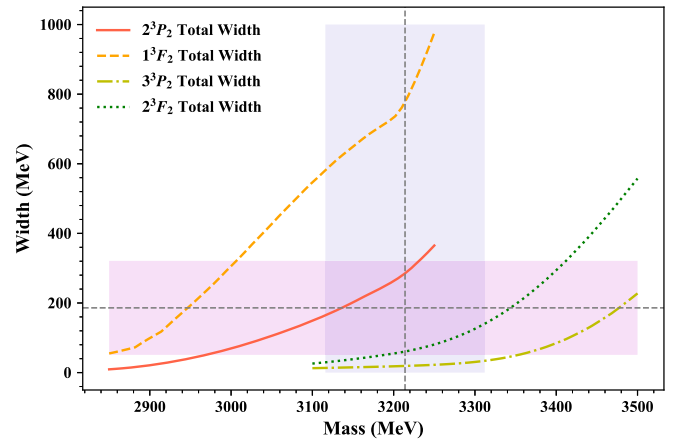
FIG. 5. Total widths change with the masses of different states for D_2^*. The vertical and horizontal dashed lines with shades are the present experimental results with errors [3].

current experimental observation [3], 2^3P_2 and 2^3F_2 states enter the error range which is denoted as the shaded area.

IV. SUMMARY

We analyzed the OZI-allowed two-body strong decay behaviors of four possible assignments of 2^+ family for the newly observed $D_2^*(3000)$. The wave functions of related charmed mesons was obtained by using the instantaneous Bethe-Salpeter method. In our calculation, $D_2^*(3000)$ as 1^3F_2 state has an exceeded width of 778 MeV, while the widths of 19.1 MeV for 3^3P_2 does not reach the lower limit. As for 2^3P_2 and 2^3F_2, the total widths are respectively 285.6 MeV and 60.5 MeV, which are in the error range of present experimental results. $D\pi$ channels are important for all four candidates, which shows consistency with the current experiment. Additionally, the channels involving $D_1(2420)/D_1(2430)$, $D_{s1}(2536)/D_{s1}(2460)$, and $D_2(2740)/D_2(2780)$, which give significant contribution and influence the mixing angle, was discussed. Our study also indicates a strong dependence between total widths and state masses. Thus, different models with varying mass input don't reach a consensus. Considering the large uncertainties of preliminary observation, besides the possible individual states, mixing of several states is also a potential option for the current $D_2^*(3000)$. More accurate measurements and theoretical efforts are expected in the future.

[1] P. A. Zyla *et al.* (Particle Data Group), Prog. Theor. Exp. Phys. **2020**, 083C01 (2020).

[2] R. Aaij *et al.* (LHCb Collaboration), J. High Energy Phys. 09 (2013) 145.

[3] R. Aaij *et al.* (LHCb Collaboration), Phys. Rev. D **94**, 072001 (2016).

[4] Y. Sun, X. Liu, and T. Matsuki, Phys. Rev. D **88**, 094020 (2013).

[5] Q.-F. Lü and D.-M. Li, Phys. Rev. D **90**, 054024 (2014).

[6] G.-L. Yu, Z.-G. Wang, Z.-Y. Li, and G.-Q. Meng, Chin. Phys. C **39**, 063101 (2015).

[7] S. Godfrey and K. Moats, Phys. Rev. D **93**, 034035 (2016).

[8] P. Gupta and A. Upadhyay, Phys. Rev. D **97**, 014015 (2018).

[9] Q.-T. Song, D.-Y. Chen, X. Liu, and T. Matsuki, Phys. Rev. D **92**, 074011 (2015).

[10] S.-C. Li, T. Wang, Y. Jiang, X.-Z. Tan, Q. Li, G.-L. Wang, and C.-H. Chang, Phys. Rev. D **97**, 054002 (2018).

[11] X.-Z. Tan, T. Wang, Y. Jiang, S.-C. Li, Q. Li, G.-L. Wang, and C.-H. Chang, Eur. Phys. J. C **78**, 583 (2018).

[12] S.-C. Zhang, T. Wang, Y. Jiang, Q. Li, and G.-L. Wang, Int. J. Mod. Phys. A **32**, 1750022 (2017).

[13] F. E. Close and E. S. Swanson, Phys. Rev. D **72**, 094004 (2005).

[14] X.-H. Zhong and Q. Zhao, Phys. Rev. D **78**, 014029 (2008).

[15] T. Matsuki and K. Seo, Phys. Rev. D **85**, 014036 (2012).

[16] D. Ebert, R. N. Faustov, and V. O. Galkin, Eur. Phys. J. C **66**, 197 (2010).

[17] J.-Z. Wang, D.-Y. Chen, Q.-T. Song, X. Liu, and T. Matsuki, Phys. Rev. D **94**, 094044 (2016).

[18] A. M. Badalian and B. L. G. Bakker, Phys. At. Nucl. **84**, 354 (2021).

[19] V. Patel, R. Chaturvedi, and A. K. Rai, Eur. Phys. J. Plus **136**, 42 (2021).

[20] R.-H. Ni, Q. Li, and X.-H. Zhong, Phys. Rev. D **105**, 056006 (2022).

[21] Z.-G. Wang, Commun. Theor. Phys. **66**, 671 (2016).

[22] G.-L. Yu, Z.-G. Wang, and Z. Li, Phys. Rev. D **94**, 074024 (2016).

[23] L.-Y. Xiao and X.-H. Zhong, Phys. Rev. D **90**, 074029 (2014).

[24] E. E. Salpeter and H. A. Bethe, Phys. Rev. **84**, 1232 (1951).

[25] E. E. Salpeter, Phys. Rev. **87**, 328 (1952).

[26] C. S. Kim and G.-L. Wang, Phys. Lett. B **584**, 285 (2004); **634**, 564(E) (2006).

[27] G.-L. Wang, Phys. Lett. B **653**, 206 (2007).

[28] G.-L. Wang, Phys. Lett. B **674**, 172 (2009).

[29] H.-F. Fu, X.-J. Chen, G.-L. Wang, and T.-H. Wang, Int. J. Mod. Phys. A **27**, 1250027 (2012).

[30] Z.-H. Wang, G.-L. Wang, J.-M. Zhang, and T.-H. Wang, J. Phys. G **39**, 085006 (2012).

[31] T. Wang, G.-L. Wang, H.-F. Fu, and W.-L. Ju, J. High Energy Phys. 07 (2013) 120.

[32] Q. Li, T. Wang, Y. Jiang, H. Yuan, and G.-L. Wang, Eur. Phys. J. C **76**, 454 (2016).

[33] Q. Li, T. Wang, Y. Jiang, H. Yuan, T. Zhou, and G.-L. Wang, Eur. Phys. J. C **77**, 12 (2017).

[34] Z.-H. Wang, Y. Zhang, L. Jiang, T.-H. Wang, Y. Jiang, and G.-L. Wang, Eur. Phys. J. C **77**, 43 (2017).

[35] Q. Li, Y. Jiang, T. Wang, H. Yuan, G.-L. Wang, and C.-H. Chang, Eur. Phys. J. C **77**, 297 (2017).

[36] T. Zhou, T. Wang, Y. Jiang, X.-Z. Tan, G. Li, and G.-L. Wang, Int. J. Mod. Phys. A **35**, 2050076 (2020).

[37] Z.-K. Geng, T. Wang, Y. Jiang, G. Li, X.-Z. Tan, and G.-L. Wang, Phys. Rev. D **99**, 013006 (2019).

[38] X.-H. Zhong and Q. Zhao, Phys. Rev. D **81**, 014031 (2010).

[39] T. Wang, Z.-H. Wang, Y. Jiang, L. Jiang, and G.-L. Wang, Eur. Phys. J. C **77**, 38 (2017).

[40] C.-H. Chang, J.-K. Chen, X.-Q. Li, and G.-L. Wang, Commun. Theor. Phys. **43**, 113 (2005).

[41] Q. Li, T. Wang, Y. Jiang, G.-L. Wang, and C.-H. Chang, Phys. Rev. D **100**, 076020 (2019).

[42] C.-H. Chang, C. S. Kim, and G.-L. Wang, Phys. Lett. B **623**, 218 (2005).

[43] S. Mandelstam, Proc. R. Soc. A **233**, 248 (1955).

[44] T. Barnes, S. Godfrey, and E. S. Swanson, Phys. Rev. D **72**, 054026 (2005).

[45] T. Matsuki, T. Morii, and K. Seo, Prog. Theor. Phys. **124**, 285 (2010).

[46] H.-Y. Cheng and C.-K. Chua, Phys. Rev. D **74**, 034020 (2006).

[47] W.-L. Ju, G.-L. Wang, H.-F. Fu, Z.-H. Wang, and Y. Li, J. High Energy Phys. 09 (2015) 171.

[48] G.-L. Wang, T. Wang, Q. Li, and C.-H. Chang, arXiv: 2201.02318.

[49] Z.-H. Wang, Y. Zhang, T.-h. Wang, Y. Jiang, Q. Li, and G.-L. Wang, Chin. Phys. C **42**, 123101 (2018).